

The *Mus musculus* papillomavirus type 1 E7 protein binds to the retinoblastoma tumor suppressor - implications for viral pathogenesis

Tao Wei^{a§}, Miranda Grace^{b§}, Aayushi Uberoi^{a*}, James C. Romero-Masters^a, Denis Lee^a, Paul F. Lambert^{a#}, Karl Munger^{b#}

^aMcArdle Laboratory for Cancer Research, University of Wisconsin School of Medicine and Public Health, Madison, WI

^bDepartment of Developmental, Molecular and Chemical Biology, Tufts University School of Medicine, Boston, MA

[§]these two authors have contributed equally

*Current address: Department of Dermatology, University of Pennsylvania, Philadelphia, PA

#Corresponding authors: Karl.Munger@tufts.edu

Plambert@wisc.edu

Running title: MmuPV1 E7 and viral pathogenesis

Keywords: Papillomavirus; viral pathogenesis, retinoblastoma tumor suppressor, E7, MmuPV1

1 **Abstract**

2 The species specificity of papillomaviruses has been a significant roadblock for performing in
3 vivo pathogenesis studies in common model organisms. The *Mus musculus* papillomavirus type
4 1 (MmuPV1) causes cutaneous papillomas that can progress to squamous cell carcinomas in
5 laboratory mice. The papillomavirus E6 and E7 genes encode proteins that establish and
6 maintain a cellular milieu that allows for viral genome synthesis and viral progeny synthesis in
7 growth-arrested, terminally differentiated keratinocytes. The E6 and E7 proteins provide this
8 activity by binding to and functionally reprogramming key cellular regulatory proteins. The
9 MmuPV1 E7 protein lacks the canonical LXCXE motif that mediates the binding of multiple viral
10 oncoproteins to the cellular retinoblastoma tumor suppressor protein, RB1. Our proteomic
11 experiments, however, revealed that MmuPV1 E7 still interacts specifically with RB1. We show
12 that MmuPV1 E7 interacts through its C-terminus with the C-terminal domain of RB1. Binding of
13 MmuPV1 E7 to RB1 did not cause significant activation of E2F-regulated cellular genes.
14 MmuPV1 E7 expression was shown to be essential for papilloma formation. Experimental
15 infection of mice with MmuPV1 virus expressing an E7 mutant that is defective for binding to
16 RB1 caused delayed onset, lower incidence, and smaller sizes of papillomas. Our results
17 demonstrate that the MmuPV1 E7 gene is essential and that targeting non-canonical activities
18 of RB1, which are independent of RB1's ability to modulate the expression of E2F-regulated
19 genes, contribute to papillomavirus-mediated pathogenesis.

20 **Importance**

21 Papillomavirus infections cause a variety of epithelial hyperplastic lesions, warts. While most
22 warts are benign, some papillomaviruses cause lesions that can progress to squamous cell
23 carcinomas and approximately 5% of all human cancers are caused by human papillomavirus
24 (HPV) infections. The papillomavirus E6 and E7 proteins are thought to function to reprogram
25 host epithelial cells to enable viral genome replication in terminally differentiated, normally

26 growth-arrested cells. E6 and E7 lack enzymatic activities and function by interacting and
27 functionally altering host cell regulatory proteins. Many cellular proteins that can interact with E6
28 and E7 have been identified, but the biological relevance of these interactions for viral
29 pathogenesis has not been determined. This is because papillomaviruses are species-specific
30 and do not infect heterologous hosts. Here we use a recently established mouse papillomavirus
31 (MmuPV1) model to investigate the role of the E7 protein in viral pathogenesis. We show that
32 MmuPV1 E7 is necessary for papilloma formation. The retinoblastoma tumor suppressor protein
33 (RB1) is targeted by many papillomaviral E7 proteins, including cancer-associated HPVs. We
34 show that MmuPV1 E7 can bind RB1 and that infection with a mutant MmuPV1 virus that
35 expresses an RB1 binding defective E7 mutant caused smaller and fewer papillomas that arise
36 with delayed kinetics.

37

38 INTRODUCTION

39 Papillomaviruses (PVs) have been isolated from a wide range of vertebrate species. They have
40 a tropism for squamous epithelia, and individual genotypes often have a marked preference for
41 infecting mucosal or cutaneous squamous epithelia. Approximately 440 human PVs (HPVs)
42 have been identified and they are phylogenetically classified into several genera (1). Among
43 these, most alpha genus HPVs preferentially infect mucosal epithelia. A group of approximately
44 15 “high-risk” alpha genus HPVs are the etiological agents of almost all cervical cancers and a
45 large percentage of other anogenital tract carcinomas as well as a growing fraction of head and
46 neck squamous cell carcinomas (SCCs), particularly oropharyngeal cancers (2, 3). Overall,
47 high-risk HPV infections contribute to >5% of all human cancers (4). The beta and gamma
48 genus HPVs mostly infect cutaneous epithelia and infections with some of these HPVs
49 contribute to the development of cutaneous squamous cell carcinomas (cSCCs) in individuals
50 afflicted by the rare hereditary disease, epidermodysplasia verruciformis (5, 6), or in long-term
51 systemically immune-suppressed organ transplant patients (7-9).

52
53 Cell- and animal model-based studies have revealed that the E6 and E7 proteins of high-risk
54 alpha, as well as the cSCC-associated beta HPVs, have oncogenic activities. HPV E6 and E7
55 encode small, cysteine-rich, metal-binding proteins. They lack intrinsic enzymatic activities, do
56 not function as DNA binding transcription factors, and do not share extensive sequence
57 similarities with cellular proteins. By binding to and interfering with the functionality of important,
58 host regulatory proteins they elicit profound alterations in cellular physiology to permit long-term
59 viral persistence as well as viral progeny synthesis (10, 11). In rare cases, these alterations and
60 the cellular responses that are triggered can cause cancer formation (12). A large number of
61 potential cellular protein targets have been identified for the high-risk alpha HPV E6 and E7
62 proteins through proteomic studies (10, 11). Similar proteomic experiments with the beta HPV

63 E6 and E7 proteins have revealed that, while they share some interactors with high-risk
64 mucosal HPVs, they also interact with distinct cellular proteins and signaling pathways (13).
65
66 Papillomaviruses are species-specific and cannot productively infect heterologous host
67 organisms. Hence the biological relevance of specific interactions of the HPV E6 and E7
68 proteins with specific host pathways cannot be tested in infectious animal models. Traditional
69 animal models of PV infection and pathogenesis are limited to species that are not genetically
70 tractable. The discovery of the *Mus musculus* papillomavirus type 1 (MmuPV1), which can be
71 used to experimentally infect standard laboratory mice, has finally provided a viable
72 experimental model system to explore the importance of specific virus-host interactions in viral
73 pathogenesis. MmuPV1 was discovered based on its ability to cause cutaneous papillomas and
74 provides us an opportunity to better understand molecular mechanisms by which HPVs promote
75 cutaneous disease in an *in vivo* animal model (14).

76
77 We have previously reported that the MmuPV1 E6 protein shares with the beta HPV8 E6 protein
78 the ability to inhibit NOTCH and TGF-beta signaling by interacting with the NOTCH co-activator
79 MAML and the DNA binding SMAD2 and SMAD3 proteins that are downstream of TGF-beta
80 signaling (15). Moreover, by experimentally infecting with MmuPV1 mutant genomes we
81 showed that the presence of a functional MAML1 binding site on E6 is critical for papilloma
82 formation (15). We have now extended these proteomic studies to the MmuPV1 E7 protein.
83 Here we show that MmuPV1 E7 expression is necessary for papilloma formation. Like some
84 gamma HPV E7 proteins, MmuPV1 E7 lacks an LXCXE (L, leucine; C, cysteine; E, glutamic
85 acid; X, any amino acid)-based binding site for the retinoblastoma tumor suppressor, RB1 (16,
86 17). Using affinity purification of MmuPV1 E7 associated cellular protein complexes followed by
87 mass spectrometry, we discovered that MmuPV1 E7 can bind RB1. Similar to some animal PV
88 and gamma HPV E7 proteins that also bind RB1 despite lacking LXCXE domains, the RB1

89 binding site maps to the MmuPV1 E7 C-terminus. Experimental MmuPV1 infection of a mouse
90 strain that expresses an LXCXE protein binding deficient RB1 mutant, causes the formation of
91 papillomas. This result shows that the ability of MmuPV1 to cause papillomas is not dependent
92 on binding RB1 through its LXCXE binding cleft. Consistent with this finding, we mapped the
93 MmuPV1 E7 binding site to the RB1 C-terminus. Unlike LXCXE containing E7 proteins,
94 MmuPV1 E7 expression did not trigger efficient activation of E2F-responsive cellular genes.
95 Experimental infection with a MmuPV1 mutant virus that encodes an RB1 binding defective E7
96 protein, inefficiently caused papillomas when compared to the wild type virus, and the lesions
97 that did arise were smaller and appeared later than those arising in wild type MmuPV1 infected
98 animals. These findings support the hypothesis that MmuPV1 E7 contributes to pathogenesis,
99 at least in part, through its interactions with RB1.

100

101 **RESULTS**

102 **MmuPV1 E7 is required for viral pathogenesis**

103 To understand how MmuPV1 mediates its pathogenesis, we first asked whether the viral E7
104 gene is required for the virus to induce papillomas. To address this question, we engineered a
105 stop codon immediately after the ATG initiation codon in the MmuPV1 E7 translational open
106 reading frame in the context of the full-length MmuPV1 DNA genome. MmuPV1 E7 only
107 contains one translational start codon, so no E7-related polypeptides can be expressed from
108 internal methionine residues. Nor have there been identified any spliced MmuPV1 mRNAs that
109 could produce E7-related polypeptide initiating from a start codon present in an upstream open
110 reading frame (18). MmuPV1 quasivirus containing the wild type or E7 stop mutant were
111 generated in vitro in 293FT cells as described previously (19). The yield of virus particles
112 containing encapsidated viral genomes was determined by quantifying the amount of DNase
113 resistant viral genomes in the fractions from the density gradient (19). These virus particles are
114 referred to as “quasiviruses” to distinguish them from authentic viruses generated in naturally

115 infected tissue. The infectivity of these viral stocks was confirmed by RT-PCR detection of viral
116 E1[^]E4 spliced mRNAs expressed at 48 hours after infecting cultured mouse keratinocytes
117 **(Figure 1A).**

118

119 Stocks of quasiviruses containing either wild type (MmuPV1) or E7-null (MmuPV1 E7^{STOP})
120 genomes were used to infect Nude-FoxN1^{nu/nu} mice at cutaneous sites, both on the ears and tail,
121 at the same dose of 10⁸ viral genome equivalents (VGE) that was shown previously to induce
122 papillomas at 100% of sites infected with wild type MmuPV1 (20). Briefly, sites were wounded
123 by lightly scarifying the epidermis with a needle, then a solution containing quasivirus was
124 applied to the wounded skin. Mice were monitored for papilloma formation weekly for 3 months.
125 As observed before (20), wild-type MmuPV1 quasivirus caused papilloma formation at 100% of
126 infected sites on the nude mice, whereas infections with the mutant MmuPV1 E7^{STOP} quasivirus
127 did not induce any papillomas **(Figure 1B)**. Mock-infected nude mice also did not develop
128 papillomas (15). The experiment was repeated by placing on wounded sites naked re-
129 circularized viral genomes, which have been reported to be infectious and cause papilloma
130 formation (13, 21). Consistent with our previous findings (15), 10 µg of re-circularized wild type
131 MmuPV1 genome caused papillomas at 100% of sites exposed to the viral DNA on the nude
132 mice by the end of 3 months post-infection, whereas 10 µg of re-circularized MmuPV1 E7^{STOP}
133 viral DNA failed to induce papillomas at any sites **(Figure 1B)**. Together, these results indicate
134 that the expression of the viral E7 protein is required for MmuPV1 to induce papillomatosis *in*
135 *vivo*.

136

137 **MmuPV1 E7 lacks an LXCXE motif but can bind to RB1**

138 The retinoblastoma tumor suppressor, RB1, is an important cellular target of many PV E7
139 proteins. Most PV E7 proteins interact with RB1 through a conserved, N-terminal LXCXE motif
140 (11). The MmuPV1 E7 protein, however, lacks an LXCXE sequence **(Figure 2A)**. Some PVs

141 including the canine papillomavirus type 2 (CPV2) and the gamma HPV4 and HPV197 E7
142 proteins have been shown to bind RB1 despite lacking LXCXE domains (16, 17). To determine
143 whether MmuPV1 E7 may bind RB1 we performed affinity purification/mass spectrometry
144 (AP/MS) experiments. N-terminal and C-terminal FLAG/HA epitope-tagged MmuPV1 E7
145 proteins were transiently expressed in HCT116 human colon carcinoma cells. HCT116 cells are
146 used because they are of epithelial origin, are highly transfectable, express wild-type RB1 and
147 do not contain any known exogenous viral sequences. MmuPV1 E7-associated proteins
148 complexes were isolated by affinity chromatography on HA antibody resin, eluted with HA
149 peptide, and analyzed by mass spectrometry. These experiments revealed that MmuPV1 E7
150 can interact with RB1 as evidenced by the detection of 34 and 16 unique RB1 peptides in
151 experiments performed with N-terminally and C-terminally tagged MmuPV1 E7, respectively
152 (Table S1). We confirmed the MmuPV1 E7/RB1 interaction by transfecting HCT116 cells with
153 an expression vector encoding N-terminally FLAG/HA-tagged MmuPV1 E7 followed by
154 immunoprecipitation/western blot analysis (**Figure 2B**). We also found MmuPV1 E7 to bind to
155 endogenous murine Rb1 in similar IP/western experiments performed in mouse NIH3T3
156 fibroblasts using transfected N-terminally FLAG/HA-tagged MmuPV1 E7 (**Figure 2C**). That
157 MmuPV1 E7 can bind both human and murine retinoblastoma proteins is not surprising; they
158 are highly conserved. Because of a lack of availability of expression vectors for murine Rb1,
159 subsequent studies characterizing the nature of this interaction, described below, were
160 necessarily carried out using expression vectors for wild-type or mutant forms of human RB1.

161

162 The canine papillomavirus 2 (CPV2) E7 protein, which, similar to MmuPV1 E7, lacks an LXCXE
163 domain, has been reported not only to bind RB1 but also to destabilize it (16). Given the
164 importance of RB1 destabilization by high-risk HPVs in cellular transformation (22), we asked
165 whether MmuPV1 E7 can destabilize RB1. RB1 was co-transfected in combination with
166 increasing amounts of MmuPV1 E7 into SAOS-2 human osteosarcoma cells, which express an

167 inactive, C-terminally truncated, barely detectable RB1 mutant (23). In contrast to HPV16 E7 (22,
168 24), expression of MmuPV1 E7 did not cause a significant decrease in RB1 steady-state levels.
169 Hence MmuPV1 does not cause detectable RB1 destabilization (**Figure 2D**).

170

171 **MmuPV1 E7 does not as efficiently activate E2F-dependent gene expression as HPV16 E7**

172 One of the best-studied biological activities of RB1 is its regulation of the activity of the
173 transcription factor E2F1 (25-27). RB1 undergoes cell cycle-dependent phosphorylation and
174 dephosphorylation. Hypophosphorylated RB1 binds to E2F family members and the resulting
175 RB1/E2F transcriptional repressor complexes restrain transition from the G1 to the S phase of
176 the cell cycle. When RB1 is hyperphosphorylated by cyclin-dependent kinases, it permits E2Fs
177 to function as transcriptional activators and drive S-phase progression (28, 29). Like adenovirus
178 E1A and polyomavirus large tumor antigens, LXCXE motif-containing HPV E7 proteins bind
179 RB1 and abrogate the formation of RB1/E2F repressor complexes thereby causing aberrant S-
180 phase entry. It is thought that this activity of the viral proteins is key to retaining infected host
181 cells in a replication-competent state that is conducive for viral genome synthesis (30). To
182 determine whether MmuPV1 binding to RB1 affects E2F transcription factor activity, we
183 determined expression levels of four well-established, E2F-regulated genes, cyclin E2 (CCNE2)
184 (31), minichromosome maintenance complex components 2 (MCM2) and 7 (MCM7) (32) as well
185 as Proliferating Cell Nuclear Antigen (PCNA) (33) in MmuPV1 E7 expressing, telomerase-
186 immortalized human keratinocytes (iHFKs) or early passage mouse keratinocytes. HPV16 E7
187 expressing cells were used as controls. While expression of CCNE2, MCM2, MCM7, and PCNA
188 was significantly increased in HPV16 E7-expressing iHFKs, there was no comparable increase
189 in the expression of these genes in MmuPV1 E7-expressing iHFKs (**Figure 3A**) or primary
190 mouse keratinocytes (**Figure 3B**). Based on these results, we conclude that MmuPV1 E7 does
191 not as efficiently activate the expression of E2F-responsive genes as HPV16 E7.

192

193 **The MmuPV1 E7 protein interacts with RB1 sequences that are distinct from the LXCXE**
194 **binding cleft**

195 Because MmuPV1 E7 does not contain an LXCXE sequence, we wanted to test whether it
196 binds RB1 similarly or distinctly to LXCXE-containing E7 proteins. The LXCXE binding site in
197 RB1 has been determined by X-ray co-crystallography studies (34). Based on this information,
198 an LXCXE binding defective RB1 mutant with amino acid substitutions at three critical contact
199 residues (I753A; N757A; M761A) (RB1^L) was constructed (35). We compared the abilities of
200 HPV16 E7, which binds RB1 through its LXCXE motif, and MmuPV1 E7 to bind to wild-type
201 RB1 versus the RB1^L mutant by expressing the corresponding proteins in SAOS-2 cells. As
202 expected (35), HPV16 E7 interacted with wild-type RB1 but not the RB1^L mutant. In contrast,
203 MmuPV1 interacted with both wild-type RB1 and mutant RB1^L with similar efficiencies. These
204 experiments reveal that MmuPV1 interacts with RB1 sequences that are distinct from those
205 necessary for interaction with LXCXE motif-containing E7 proteins (**Figure 4**).

206

207 **MmuPV1 causes warts in mice expressing the LXCXE binding defective Rb1^L mutant**

208 We previously used *Rb1^L* knock-in mice expressing the above described mutant Rb1 to
209 investigate the role of HPV16 E7's binding to Rb1 in neoplastic disease (36, 37). Given that
210 MmuPV1 E7 can interact with the RB1^L, we asked if MmuPV1 can cause disease in *Rb1^L* mice.
211 Ears of both wild-type *FVB* and *Rb1^L FVB* mice were infected with 10⁸ VGE of MmuPV1 (virus
212 stock generated from MmuPV1-induced warts from a nude mouse - see Materials and Methods)
213 as described previously (20) using the same methodology used in our previous experiments for
214 quasivirus infections. By the end of 4 months, MmuPV1 caused a similar incidence of
215 papillomas in both the wild type and *Rb1^L FVB* mice (**Figure 5A**, *p-value* = 1, two-sided Fisher's
216 exact test). There was no apparent size difference between warts from the MmuPV1-infected
217 wild-type mice and those from *Rb1^L* mice, based on H&E analysis (data not shown).

218

219 We next performed immunohistochemistry on tissues obtained at the experimental endpoint to
220 compare the expression of biomarkers for viral infection between the papillomas arising in wild
221 type and *Rb1^L FVB* mice (**Figure 5B**). Ki67-specific immunohistochemistry showed similar
222 levels of cell proliferation in the papillomas arising on both the wild type and *Rb1^L FVB* mice.
223 MCM7 was also upregulated to similar levels, indicating that MmuPV1 is capable of increasing
224 E2F-driven gene expression despite the disruption in the LXCXE binding cleft in the *Rb1^L FVB*
225 mice. These results demonstrate that the disruption of the ability of RB1 to bind proteins via
226 their LXCXE-motifs is not required for MmuPV1 to induce papillomas or to induce expression of
227 E2F-responsive genes.

228

229 **C-terminal RB1 sequences are necessary for interaction with MmuPV1 E7**

230 Given that MmuPV1 E7 does not interact with the LXCXE binding cleft of RB1 we mapped the
231 RB1 region responsible for binding MmuPV1 E7. We co-expressed MmuPV1 E7 with plasmids
232 expressing full-length RB1 (amino acid residues 1-928) or truncation mutants of RB1 lacking the
233 amino-terminus (amino acid residues 379-928) or the C-terminus (amino acid residues 1-792) in
234 SAOS2 human osteosarcoma cells. HPV16 E7 was used as a control. As expected, HPV16 E7
235 efficiently bound wild-type RB1, as well as the two truncation mutants, both of which encode the
236 A and B domains of RB1 that contain the LXCXE binding cleft. In contrast, MmuPV1 E7 did not
237 efficiently interact with the 1-792 mutant RB1 that lacks the C-terminal domain of RB1 (**Figure**
238 **6A, B**). Hence MmuPV1 E7 primarily interacts with the C-terminal domain of RB1.

239

240 **C-terminal MmuPV1 E7 sequences are necessary for RB1 binding**

241 It has previously been reported that the E7 proteins of CPV2 and HPV4, which also lack LXCXE
242 motifs in their N-termini, associate with RB1 through their C-termini (16). Hence, in addition to
243 testing some mutations in the N-terminus of MmuPV1 E7, we also generated MmuPV1 E7
244 mutants in the C-terminal domain. We focused on regions that are conserved between CPV2,

245 HPV4, HPV197, and MmuPV1 (**Figure 7A**). Of all the mutants that were tested, a four amino
246 acid deletion of residues 84 to 87 (MmuPV1 E7^{Δ84-87}) and an alanine substitution at aspartate
247 residue 90 (MmuPV1 E7^{D90A}) were found to be defective for RB1 binding (**Figure 7B**). Based on
248 these results we generated two additional substitution mutants, MmuPV1 E7^{D90T} and MmuPV1
249 E7^{D90N}. MmuPV1 E7^{D90T} was generated to mimic the HPV16 E7 threonine residue at this
250 position (**Figure 7A**). MmuPV1 E7^{D90T} displayed decreased RB1 binding similar to MmuPV1
251 E7^{D90A}. The MmuPV1 E7^{D90N} mutant, which was generated to neutralize the negative charge
252 while maintaining the general architecture of the side chain, retained some binding to RB1, even
253 though it was expressed at lower levels than the other two mutants (**Figure 7C**). Lastly, the
254 MmuPV1 E7^{D90A} mutant was also defective for binding to murine Rb1 (**Figure 7D**). Hence,
255 similar to CPV2 and gamma-HPVs (16), MmuPV1 E7 binds to RB1 through its C-terminal
256 domain, and based on the results described above, we chose the MmuPV1 E7^{D90A} mutant for
257 our follow-up studies.

258

259 **Reduced incidence and smaller sized warts in MmuPV1 E7^{D90A} infected mice**

260 To assess whether E7's ability to bind Rb1 contributes to MmuPV1 pathogenesis, we introduced
261 the D90A mutation into the complete MmuPV1 DNA genome which we used to make quasivirus
262 particles in 293FT cells. We then characterized the ability of this mutant MmuPV1 versus wild-
263 type MmuPV1 to cause papillomatosis in mice. Quasivirus stocks were confirmed to be
264 infectious (**Figure 8A**), by exposing mouse keratinocytes to the quasiviruses and 48 hours later
265 harvesting RNA to detect the presence of viral E1^ΔE4 spliced transcripts by RT-PCR. We then
266 performed *in vivo* infections with these stocks of infectious quasivirus. 6-8 weeks old Nude-
267 *FoxN1^{nu/nu}* mice were scarified on their ears and tails and infected with wildtype MmuPV1 or
268 E7^{D90A} mutant MmuPV1 quasivirus at doses of either 10⁷ (stock 2) or 10⁸ VGE (stock 1).
269 Papilloma incidence was monitored biweekly for 4 months. At the endpoint, wild-type MmuPV1
270 at the 10⁸ VGE dose caused papillomas at 100% of the sites infected. In contrast, the same

271 dose of MmuPV1 E7^{D90A} quasivirus caused papillomas at a significantly lower frequency, 12%
272 (**Figure 8B**, $p < 0.0001$, two-sided Fisher's exact test). At the lower 10^7 VGE dose, wild-type
273 MmuPV1 caused papillomas at a 65% frequency, whereas MmuPV1 E7^{D90A} caused papillomas
274 in only 8% of infected sites (**Figure 8B**, $p < 0.001$, two-sided Fisher's exact test). At both doses,
275 the papillomas arising on mice infecting with MmuPV1 E7^{D90A} appeared at later time points
276 (**Figure 8C**, MmuPV1 (10^8 VGE) vs. MmuPV1 E7^{D90A} stock 1, $p < 0.0001$; MmuPV1 (10^7 VGE)
277 versus MmuPV1 E7^{D90A} stock 2, $p < 0.0001$ two-sided LogRank test). At the 4 month endpoint,
278 we harvested the papillomas from all infected mice, fixed and serially sectioned the lesion, and
279 performed H&E staining. We performed scans of the H&E-stained sections from 6
280 representative papillomas induced by MmuPV1 (3 from 10^8 VGE and 3 from 10^7 VGE), and 3
281 papillomas induced by MmuPV1 E7^{D90A} quasiviruses (we scanned all three papillomas that
282 arose on mice infected with the MmuPV1 E7^{D90A} quasivirus, regardless of virus dose) (**Figure**
283 **8D**). The size of each papilloma was assessed using ImageScope under the same
284 magnification (**Figure 8E**). Papillomas caused by the MmuPV1 E7^{D90A} quasivirus were
285 significantly smaller when compared to those caused by MmuPV1 (MmuPV1 versus MmuPV1
286 E7^{D90A}, $p = 0.003$, two-sided T-test), indicating that the loss of E7's ability to interact with Rb1
287 correlates with reduced size of MmuPV1-induced papillomas. We harvested and sequenced the
288 MmuPV1 genomes present in warts arising from mice infected with the wild type and the E7^{D90A}
289 quasiviruses and confirmed that warts indeed contained the expected virus and that no cross-
290 contamination had occurred. Together, the assessments of the incidence of papillomas, the time
291 of onset of papillomas, and the size of papillomas at the endpoint all indicate that the interaction
292 between MmuPV1 E7 and Rb1 quantitatively correlates with the MmuPV1's ability to cause
293 papillomatosis.

294

295 **MmuPV1 E7^{D90A} - induced papillomas display similar histological features as papillomas**
296 **induced by wild-type MmuPV1.**

297 To determine whether the papillomas caused by MmuPV1 E7^{D90A} displayed similar or different
298 microscopic features compared to those caused by wild-type MmuPV1, we performed
299 immunohistochemistry to assess the expression of biomarkers for papillomavirus-associated
300 lesions. Evidence for productive viral infections within the papillomas was scored by performing
301 immunofluorescence staining to detect the viral capsid protein L1 (**Figure 9**, panel B). L1
302 expression was similar in papillomas induced by the wild type and mutant quasiviruses.
303 Papillomas induced by wild type and E7^{D90A} quasiviruses also showed similar patterns of
304 keratinocyte differentiation with cytokeratin 14 upregulated in the suprabasal layers of the
305 papillomas (**Figure 9**, panel B), indicating similar delays in terminal differentiation. MCM7, an
306 E2F-responsive gene that is upregulated in papillomavirus-related lesions caused by high-risk
307 HPV (38) and MmuPV1 (39) infections, was similarly upregulated in papillomas induced by wild
308 type and E7^{D90A} quasiviruses, indicating increased levels of E2F-mediated transcription in both
309 cases (Figure 9, panel C). The incorporation of BrdU into genomic DNA is often upregulated in
310 papillomavirus-related lesions as a consequence of increased DNA synthesis. Both MmuPV1
311 and MmuPV1 E7^{D90A} - induced papillomas showed increased levels of BrdU, with no obvious
312 differences in abundance or localization of BrdU-positive cells within the papillomas, indicating
313 similarly enhanced levels of DNA synthesis (**Figure 9**, panel D). Based on the biomarkers
314 tested, there were no significant differences in the histopathological features due to the loss of
315 interaction between E7 and Rb1.

316

317 **DISCUSSION**

318 The species specificity of papillomaviruses has greatly limited studies of how specific
319 biochemical activities of individual viral proteins contribute to viral pathogenesis in a natural
320 infection model. The discovery of MmuPV1 and its ability to infect and cause papillomas in
321 laboratory mice has removed this barrier. MmuPV1 is a member of the Pi genus, which

322 encompasses rodent PVs (1) and is most related to the cutaneous beta- and gamma-genus
323 HPVs (40).

324 The MmuPV1 E6 and E7 proteins share sequence similarities to cutaneous beta- and gamma-
325 HPVs, respectively (41). We have previously reported that MmuPV1 E6 is necessary for
326 papilloma formation in experimentally infected mice (15). MmuPV1 E6 shares key cellular
327 targets and biological activities with the beta-HPVs 5 and 8 E6 proteins that affect key tumor
328 suppressor gene functions, including the ability to bind the NOTCH transcriptional coactivator
329 MAML1 and the SMAD2 and SMAD3 mediators of transforming growth factor-beta (TGF-beta)
330 signaling (15). In particular, we have shown that MmuPV1 E6's ability to bind NOTCH correlates
331 with MmuPV1's ability to cause disease (15).

332 Here we show that similar to what we previously reported for E6 (15), MmuPV1 E7 is also
333 necessary for papilloma formation. Like CPV2 E7 and some gamma-HPV E7 proteins, the
334 MmuPV1 E7 protein lacks an N-terminal LXCXE motif, which is present in multiple viral and
335 cellular proteins where it serves as the binding site for members of the retinoblastoma tumor
336 suppressor family (40). We provide evidence that MmuPV1 E7 can bind to both the human and
337 murine retinoblastoma tumor suppressor proteins. We determined that the RB1 binding site is
338 located in the MmuPV1 E7 C-terminal domain, similar to CPV2 and gamma-HPV4 E7 proteins
339 (16). We identified a C-terminal mutant, MmuPV1 E7^{D90A}, that was markedly reduced for RB1
340 binding. The HPV16 E7 C-terminus may also contain a low-affinity RB1 binding site (42) and
341 mutation of the T86 residue in HPV16 E7 (which corresponds to MmuPV1 E7 D90) to an
342 aspartate (as present in MmuPV1) did not significantly affect RB1 binding in a yeast two-hybrid
343 format (43), whereas the MmuPV1 E7 E7^{D90T} mutant exhibited decreased RB1 binding. Infection
344 with the MmuPV1 E7^{D90A} mutant revealed that RB1 binding correlates with MmuPV1's ability to
345 promote efficient papilloma formation in the cutaneous infection model. However, it does not
346 appear to be essential for pathogenesis as small warts did arise, albeit at significantly reduced

347 efficiency and with a later time of onset. There is precedence for these findings as studies that
348 were done in cottontail rabbit PV (SfPV1, a.k.a. CRPV1) found E7 to be essential for promoting
349 disease (44, 45) but that E7's ability to interact with RB1, albeit through an LXCXE sequence
350 (46), is not essential for inducing papillomas in experimentally infected rabbits (47). In addition,
351 studies with transgenic mice have also provided evidence that HPV16 E7 can cause
352 hyperproliferation in mice that express the *Rb1^L* mutant, which HPV16 E7 is unable to bind (36,
353 37). Therefore, it is likely that other biological activities of PV E7 are also playing important roles
354 in promoting disease across various PVs.

355 PV E7 proteins with an LXCXE motif bind to a shallow cleft within the RB1 B "pocket" domain
356 (34). In contrast, MmuPV1 E7 interacts with the RB1 C-terminal domain. Consistent with these
357 results, experimental MmuPV1 infection of mice engineered to express the *Rb1^L* allele, in which
358 the LXCXE binding cleft in the B domain is mutated, caused papilloma formation at a similar
359 efficiency as mice infected with wild type MmuPV1 genomes. The RB1 C-terminal domain is
360 highly conserved amongst RB1 proteins from different species and is necessary for RB1 to
361 induce permanent G1 growth arrest and senescence (48-50). It has been shown to mediate
362 interactions with several different cellular proteins, including the ABL1 non-receptor tyrosine
363 kinase (51), the F-box protein SKP2 (52) and a non-canonical E2F1 complex that contains the
364 lysine methyltransferase EZH2 (53, 54). It has been reported that ABL1 selectively binds to
365 hypophosphorylated RB1 and that RB1 binding inhibits ABL1 enzymatic activity (51). While the
366 RB1 C-terminus is necessary, the ABL1 binding sequences have not been mapped in detail and
367 the biological relevance of the RB1/ABL1 interaction has remained enigmatic. SKP2 is an F-box
368 protein that is part of the cullin1 based ubiquitin ligase complex that has been shown to control
369 the degradation of the CDK2 inhibitor, p27^{KIP1} (CDKN1B). SKP2 is rapidly degraded during G1,
370 when RB1 is hyperphosphorylated, by CDH1 containing anaphase-promoting complex or
371 cyclosome (APC/C^{CDH1}) (55) that binds to RB1's A-B pocket. However, when RB1 gets

372 hyperphosphorylated, APC/C^{CDH1} dissociates from RB1 which leads to SKP2 degradation of
373 p27^{KIP1} and increased CDK2 activity which promotes S-phase entry. These and other non-
374 canonical RB1 activities (56) including the ability of RB1 to interact with E2F1/EZH2 complexes
375 that are not involved in cell cycle regulation are likely targeted by MmuPV1 E7, but further
376 studies are necessary to identify the specific target(s) and to delineate the molecular
377 consequences of C-terminal RB1 binding.

378 Given that phosphorylation-specific RB1 binding and release of E2F transcription factor
379 complexes involve RB1 sequences within the A-B domain (57, 58), and that MmuPV1 E7
380 interacts with RB1 C-terminus, it was not surprising that MmuPV1 E7 expression did not cause
381 efficient activation of E2F-responsive genes. Nevertheless, MmuPV1 can induce expression of
382 MCM7, a strongly E2F-responsive gene, in vivo in the context of papillomas it induces. We also
383 observed MCM7 induction in MmuPV-1-induced papillomas arising in mice expressing the *Rb1*^L
384 allele and in papillomas arising in animals infected with MmuPV1 genomes expressing the RB1
385 binding defective E7^{D90A} mutant. This raises the interesting question: which MmuPV1 protein(s)
386 is responsible for the increased MCM7 expression. Experiments performed with HPVs in cell
387 and transgenic animal-based models have all suggested that this activity is provided by E7 and
388 is based on its ability to inactivate RB family members and it is possible that E7^{D90A} mutant
389 retains low-level RB1 binding that may be sufficient to cause some expression of E2F-
390 responsive genes in vivo. However, our study is not the first to document E7 independent
391 induction of hyperproliferation. Experimental infection of rabbits with an SfPV1 mutant virus that
392 expressed an RB binding-deficient E7 mutant still caused the emergence of papillomas (47).
393 Our work is entirely consistent with this observation; moreover, our studies provide no evidence
394 that MmuPV1 E7 can efficiently activate the expression of E2F-responsive genes. It is possible
395 that MmuPV1 encodes another protein that can activate E2F-dependent promoters through
396 direct or indirect mechanisms. MmuPV1 E6 has been hypothesized to be able to bind Rb1 (59)

397 because it contains an LXCXE motif (L₆₇ACKE₇₁) in between its two (CXXC)₂ zinc-binding
398 domains; however, our prior AP/MS experiments failed to provide any evidence that MmuPV1
399 E6 binds to any of the RB family members (13). Another possibility is that the expression of
400 E2F-responsive genes in the papillomas reflects the ability of MmuPV1 E6 to impede
401 keratinocyte differentiation through its inhibition of NOTCH and TGF-beta signaling which may
402 help MmuPV1 infected cells maintain a proliferative state (15). Regardless, given that MmuPV1
403 E7 expression is necessary for papilloma formation, it will be important to determine the
404 mechanism by which MmuPV1 E7 contributes to papilloma formation. Infections with an RB1
405 binding defective E7 mutant gives rise to smaller papillomas with lower efficiency and delayed
406 kinetics compared to papillomas caused by wild-type MmuPV1 infection. It will be important to
407 determine whether papillomas that express the RB1 binding defective E7 mutant progress to
408 cancer at a similar frequency, or at all, compared to papillomas caused by wild-type MmuPV1.

409 In summary, our results show that loss of RB1 binding by MmuPV1 E7 correlates with a
410 quantitative defect in papilloma induction. Hence MmuPV1 E7 binding to RB1's C-terminal
411 domain remains an important mechanism by which MmuPV1 promotes disease. The integrity of
412 the RB1 C-terminus is important for many activities of RB1, but whether or how any of these
413 contribute to Rb1's tumor suppressor activity is largely unknown. Given, the vast majority of
414 studies on RB1 have focused on its ability to control E2F transcription factor activity, which is
415 shared with other RB family members that are not frequently mutated in tumors, it is unlikely
416 that regulation of E2F transcription factor activity is the sole tumor-suppressive function of RB1.
417 It will be important to rigorously determine which specific function of RB1's C-terminus
418 MmuPV1E7 disrupts. Such studies promise to provide exciting new insights into the molecular
419 basis of RB1's tumor suppressor activity.

420

421 **MATERIALS AND METHODS**

422 **Cells**

423 U2OS human osteosarcoma cells were obtained from ATCC and grown in Dulbecco's Modified
424 Eagle Medium (DMEM; Invitrogen) supplemented with 10% fetal bovine serum (FBS). SAOS-2
425 human osteosarcoma cells were obtained from ATCC and grown in McCoy's 5A medium
426 (Invitrogen) supplemented with 15% FBS. HCT116 human colon carcinoma cells were obtained
427 from ATCC and grown in McCoy's 5A medium (Invitrogen) supplemented with 10% FBS. NIH
428 3T3 murine fibroblasts were obtained from the ATCC and grown in DMEM (Invitrogen)
429 containing 5% FBS. JB6 mouse keratinocytes (gift from Dr. Nancy H. Colburn, NCI) were
430 maintained in DMEM containing 5%FBS. 293FT cells (ATCC) were maintained in DMEM with
431 10%FBS and 300 µg/mL neomycin (G418). Telomerase-immortalized human foreskin
432 keratinocytes CI398 (iHFK) (60) were a kind gift from Aloysius Klingelhutz (U. of Iowa.). iHFK
433 lines expressing various E7 proteins were established by transducing iHFKs with the
434 corresponding pLenti-NmE7 expressing lentiviruses, followed by selecting with 3 µg/ml
435 Blasticidin (RPI Research Products International, Mount Prospect, IL) for 7 days starting at two
436 days post-infection. Mouse Keratinocytes were isolated from the skin of neonate pups. After
437 incubation in PBS containing 10% antibiotics for 2 minutes, skin pieces were incubated in 0.25%
438 trypsin overnight at 4°C. The epidermis was then separated from the dermis using sterile
439 forceps, minced with a single edge razor blade, and then stirred for 1 hour at 37°C in F-media
440 (61) to generate a single-cell suspension. The cells were strained using 0.7 µm membrane
441 (102095-534; VWR), and cultured in F-media (62) containing 10 µM Y-27632 Rho-kinase
442 inhibitor (63) in the presence of mitomycin C (M4287; Sigma) treated 3T3 J2 fibroblasts. Early
443 passage cells were infected with the recombinant lentiviral or retroviral vectors expressing
444 HPV16 E7 or MmuPV1 E7, respectively, in F-medium in the absence of Y-27632 and 3T3 J2
445 feeders and re-infected after 24 hours. At 72 hours after the first infection, cells were selected

446 with the appropriate antibiotics. After selection, cells were maintained in F-media containing 10
447 μ M Y-27632 and mitomycin C-treated 3T3 J2 fibroblasts.

448

449 **Plasmids and antibodies**

450 The MmuPV1 E7 ORF was PCR amplified from the MmuPV1 genome and cloned into N- or C-
451 terminal FLAG/HA-CMV (64) and untagged pCMV-BamNeo (65) plasmids. Mutant MmuPV1 E7
452 constructs were generated by site-directed mutagenesis of N-FLAG/HA-mE7-CMV. pLenti-N-
453 mE7 was generated by Gateway cloning (Invitrogen) of PCR-amplified mE7 into pLenti 6.3/V5
454 DEST (Invitrogen). The RB1-truncation plasmids pSG5-HA-Rb 1-928, 1-792, and 379-928 were
455 kind gifts from Bill Sellers (Broad Institute). The pFADRB and pFADRB_L plasmids were kindly
456 provided by Fred Dick (Western University, Ontario). Other plasmids used were pLXSN HPV16
457 E7 (66), pCMV-Rb (67) (obtained from Phil Hinds, Tufts), CMV-C-16E7 (17), pBABE puro (68),
458 and pEGFP-C1 (Clontech). The following primary antibodies were used for
459 immunoprecipitations and western blotting: beta-Actin (MAB1501; Millipore), FLAG (F3165;
460 Sigma), GFP (9996; Santa Cruz), HA (ab9110; Abcam), RB1 (Ab-5, OP66; Millipore), and Rb1
461 (SC-74570, Santa Cruz). Secondary anti-mouse or anti-rabbit antibodies conjugated to
462 horseradish peroxidase were from GE Healthcare.

463

464 **Immunological Methods**

465 Affinity purification/mass spectrometry analyses of MmuPV E7 were performed as previously
466 described (17). HCT116 cells were transfected using Polyethylenimine (PEI) (69). At 48 hr post-
467 transfection cells were harvested in EBC buffer (50mM Tris-Cl pH 8.0, 150 mM NaCl, 0.5% NP-
468 40 and 0.5mM EDTA) supplemented with protease inhibitors (Pierce). Anti-Hemagglutinin (HA;
469 Sigma) or anti-Flag epitope (Sigma) antibodies coupled to agarose beads were used for
470 immunoprecipitations followed by SDS-PAGE and western blot analysis on PVDF membranes.
471 After incubation with appropriate primary and secondary antibodies, blots were visualized by

472 enhanced chemiluminescence and images captured using a Syngene ChemiXX6 imager with
473 Genesys software version 1.5.5.0. Signals were quantified with Genetools software version
474 4.03.05.0.

475

476 **RB1 Degradation assays**

477 RB1 degradation assays were performed as previously described (22). SAOS-2 cells were
478 transfected with CMV-RB and varying amounts of pCMV N-FLAG/HA mE7. pCMV-C16 E7 was
479 used as positive control and pEGFP-C1 was co-transfected to assess transfection efficiency. At
480 48 hours post-transfection cells were lysed in EBC and samples containing 100 µg protein were
481 subjected to western blot analysis as described above.

482

483 **Quantitative Reverse Transcription PCR**

484 RNA was isolated from pLenti-N-FLAG/HA mE7, iHFK pLenti-C-FLAG/HA-16E7, and pLenti-N-
485 GFP infected iHFKs and pLenti-N-FLAG/HA mE7, pLXSP-16E7 or control vector infected
486 primary mouse keratinocytes with the Quick-RNA Miniprep kit (Zymo Research). cDNA was
487 synthesized with the Quantinova Reverse Transcription Kit (Qiagen). Quantitative PCR was
488 performed in triplicate on a Step One Plus (Applied Biosystems) thermocycler using Fast SYBR
489 Green Master Mix (Applied Biosystems). PCR primers are listed in supplemental Table S2.
490 Target expression levels were normalized to GAPDH expression.

491

492 **Animals**

493 Immunodeficient Athymic Nude-*FoxN1^{nu/nu}* mice were purchased from Envigo. *RB1^L* mutant
494 mice were maintained on the FVB background and genotyped as published previously (37, 70).
495 Mice were housed in the Association for Assessment of Laboratory Animal Care-approved
496 McArdle Laboratory Animal Care Unit. All procedures were carried out in accordance with an

497 animal protocol approved by the University of Wisconsin Institutional Animal Care and Use
498 Committee (IACUC; protocol number M005871).

499

500 **Infection of nude mice with MmuPV1 quasiviruses**

501 MmuPV1 quasiviruses (wild type, E7^{STOP}, E7^{D90A}; note that the term “quasivirus” is used in the
502 papillomavirus field to identify a virus that is generated in cells by co-transfection of viral
503 genomes with a plasmid that expresses the viral capsid proteins) were generated as described
504 before (15). Briefly, 293FT cells were transfected with a MmuPV1 capsid protein expression
505 plasmid (71, 72) and the re-circularized genome, either from plasmids containing the wild type
506 or mutant MmuPV1 genomes. After incubation at 37 °C for 48 hours, cells were harvested and
507 virus extracted. The amount of packaged viral DNA in the stocks of quasiviruses was quantified
508 by Southern blotting allowing us to define the ‘viral genome equivalents” (VGE), as a measure
509 of virus concentration in each stock. The quasiviruses were used to infect Nude-*FoxN1*^{nu/nu} mice
510 as previously described (15). Briefly, animals were placed under anesthesia and infected by first
511 scarifying the epidermis using a 27-gauge syringe needle and then pipetting onto the wounded
512 site the indicated amount of quasivirus using a siliconized pipette tip. Each mouse was infected
513 at 5 sites maximum (one site per ear, three sites on tail). Papillomatosis was monitored weekly/
514 bi-weekly as indicated.

515

516 **Infection of FVB-background mice with MmuPV1**

517 The infection method has been described previously with some modifications (20). Briefly, under
518 anesthesia, mouse ears of both FVB and *RB1*^L mutant mice were scarified first using 27-gauge
519 syringe needles and infected with 10⁸ VGE/site of a pre-prepared stock of MmuPV1 virus
520 generated from a MmuPV1-infected wart. 24 hours later, mice were exposed to 300mJ UVB
521 (Daavlin, Bryan, OH). Papillomatosis was monitored over 4 months.

522

523 **RT-PCR to detect MmuPV1 E1^{E4} spliced transcripts**

524 Mouse keratinocytes JB6 cells were infected with MmuPV1 wild type and mutant quasiviruses at
525 10⁸ VGE, and changed to fresh media 3 hours later. After incubation at 37°C for 48 hours, total
526 RNA was extracted from infected JB6 cells using the RNeasy kit (Qiagen) and reverse-
527 transcribed into cDNA using the QuantiTect Reverse Transcription Kit (Qiagen). E1^{E4}
528 transcripts were detected by PCR, using p53 as a positive control. Primer sequences were
529 described previously (72).

530

531 **BrdU incorporation**

532 To evaluate levels of DNA synthesis, we performed bromodeoxyuridine (BrdU) incorporation by
533 injecting BrdU (Sigma, dissolved in PBS to 12 mg/ml stock concentration, keep at -20°C). Mice
534 were intraperitoneally injected with 250 µl stock BrdU one hour before harvest. Tissues were
535 harvest and processed for immunohistochemistry using a BrdU-specific antibody (203806,
536 Calbiochem) as previously described (15).

537

538 **Histological analysis**

539 Tissues were harvested and fixed in 4% paraformaldehyde (in PBS) for 24 hours, then switched
540 to 70% ethanol for 24 hours, processed, embedded in paraffin, and sectioned at 5 µm intervals.
541 Every 10th section was stained with hematoxylin and eosin (H&E).

542

543 **MmuPV1 L1-cytokeratin dual immunofluorescence and Immunohistochemistry**

544 L1 signals were detected using a tyramide-based signal amplification (TSA) method (73). A
545 detailed protocol is available at: <https://www.protocols.io/view/untitled-protocol-i8cchsw>.

546 For immunohistochemistry, tissue sections were deparaffinized in xylenes and rehydrated in
547 100%, 95%, 70%, and 50% ethanol, then in water. Antigen unmasking was performed by
548 heating with 10 mM citrate buffer (pH=6) for 20 minutes. Blocking was performed with 2.5%

549 horse serum in PBST for 1 hour at room temperature (RT). Slides were incubated in primary
550 antibody (BrdU; MCM7, Thermo Scientific, Fremont, CA) at 4°C, overnight in a humidified
551 chamber. M.O.M.® ImmPRESS® HRP (Peroxidase) polymer kit (Vector, MP-2400) was applied
552 the next day for 1 hour at RT for secondary antibody incubation. Slides were then incubated
553 with 3,3'-diaminobenzidine (Vector Laboratories), and counterstained with hematoxylin. All
554 images were taken with a Zeiss AxioImager M2 microscope using AxioVision software version
555 4.8.2.

556

557 **Full scan for wart size measurement, and statistical analysis**

558 Full scans of representative warts were performed by the UW Translational Research Initiatives
559 in Pathology (TRIP) facility. Measurements were performed on the full-scanned images using
560 ImageScope software (v12.4.0). All statistical analyses were performed using MSTAT statistical
561 software version 6.4.2 (<http://www.mcardle.wisc.edu/mstat>).

562

563 **ACKNOWLEDGMENTS**

564 We thank Dr. Al Klingelutz (University of Iowa) for providing telomerase immortalized human
565 foreskin keratinocytes, members of the Lambert and Munger labs for stimulating discussion and
566 valuable suggestions throughout the course of this work, Ella Ward-Shaw for expert
567 histotechnology assistance, and Simon Blaine-Sauer for isolating C57/B6 mouse keratinocytes
568 from neonates. Supported by PHS grant R01 CA228543 (K.M. and P.F.L.) and a Ruth L.
569 Kirschstein Postdoctoral Individual National Research Service Award F32 CA254019 (J.R.).

570

571 **FIGURE LEGENDS:**

572

573 **Figure 1. MmuPV1 lacking E7 expression does not induce warts.** The MmuPV1 E7^{STOP}
574 quasivirus is infectious. To assess infectivity of quasivirus stocks, mouse JB6 keratinocytes
575 were exposed to quasivirus and 48 hours later RNA was extracted and subjected to reverse
576 transcription-coupled polymerase chain reaction to detect MmuPV1 E1^{E4} transcripts (top
577 panel). GAPDH expression is shown as a control (bottom panel). Samples were run on the
578 same gel, with irrelevant lanes in the middle cropped out in **(A)**. Tails and ears of nude mice
579 were scarified and infected with the indicated amounts of quasiviruses or DNA and monitored
580 for wart formation over 3 months. Neither MmuPV1 E7^{STOP} quasivirus nor MmuPV1 E7^{STOP} DNA
581 induced wart formation, while wild type MmuPV1 quasivirus or DNA induced warts with a 100%
582 penetrance **(B)**.

583

584 **Figure 2. MmuPV1 E7 binds but does not destabilize the retinoblastoma tumor**
585 **suppressor protein, RB1.** Alignment of the N-terminal sequences of MmuPV1 E7 and the
586 canine papillomavirus 2 (CPV2), γ 1-HPV4, γ 24-HPV197, β 1-HPV8, and α 9-HPV16. Identical
587 residues are marked by black boxes, chemically similar residues are shaded in gray. The
588 position of the LXCXE RB1 binding site is highlighted. A cartoon of the domain structure of E7 is
589 shown on top, with the N-terminal sequences that show similarity the conserved regions 1 and
590 2 (CR1, CR2) of adenovirus E1A proteins indicated **(A)**. MmuPV1 E7 (M E7) can interact with
591 RB1 by immunoprecipitation/immunoblot analysis. Duplicate cultures of HCT116 cells were
592 transfected with an N-terminally HA/FLAG epitope-tagged MmuPV1 E7 expression plasmid and
593 co-precipitated RB1 protein detected by immunoblotting **(B)**. MmuPV1 E7 (M E7) can interact
594 with murine Rb1 by immunoprecipitation/immunoblot analysis. NIH 3T3 murine fibroblasts were
595 transfected with an N-terminally HA/FLAG epitope-tagged MmuPV1 E7 expression plasmid and
596 co-precipitated RB1 protein detected by immunoblotting **(C)**. MmuPV1 E7 does not destabilize

597 RB. SAOS-2 human osteosarcoma cells that do not express detectable endogenous RB were
598 transfected with an RB expression vector and increasing amounts of an expression vector for N-
599 terminally HA/FLAG epitope-tagged MmuPV1 followed by western blotting to assess RB1
600 steady levels by western blotting. GFP was co-transfected and assessed by western blotting to
601 control for transfection efficiency. HPV16 E7 (16 E7) was used as a positive control. A
602 representative blot from one of four experiments is shown **(D)**.

603

604 **Figure 3. MmuPV1 E7 does not efficiently activate E2F-regulated genes.** Expression
605 of E2F target genes, cyclin E2 (CCNE2), Minichromosome Maintenance Complex Components
606 2 and 7 (MCM2, MCM7) and Proliferating Cell Nuclear Antigen (PCNA) in immortalized human
607 foreskin keratinocytes (iHFKs) **(A)**, or in primary mouse keratinocytes (MK) **(B)** transduced with
608 control vector (C), MmuPV1 E7 (M E7) or HPV16 E7 (16 E7) as determined by quantitative
609 reverse transcription-coupled polymerase chain reaction analysis (****, $p < 0.001$; ***, $p < 0.005$;
610 n.s. not significant).

611

612 **Figure 4. The LXCXE binding cleft in the RB1 protein is not necessary for MmuPV1**
613 **E7 binding.** SAOS-2 human osteosarcoma cells were transfected with expression vectors for
614 wildtype RB1 or the RB1^L mutant that contains three amino acid mutations in the LXCXE
615 binding cleft in combination with MmuPV1 or HPV16 E7 expression vectors. MmuPV1 E7 binds
616 wild type and RB1^L with similar efficiency whereas HPV16 E7 binds and causes degradation of
617 RB1 but not RB1^L. The results shown are representative of two independent experiments. A
618 cartoon of the RB1^L mutant is shown at the top of the figure.

619

620 **Figure 5. Disruption of the LXCXE binding cleft in RB1 does not influence MmuPV1's**
621 **ability to cause papillomas in vivo.** Sites on the ears of both wild-type and RB1^L mutant
622 FVB/N mice were scarified and infected with 10^8 VGE of MmuPV1. Mice were treated with 300

623 mJ UVB the next day and then monitored for papilloma formation over 4 months. MmuPV1
624 induced warts in wild type and RB1^L mutant FVB/N mice with a similar incidence (Fisher's exact
625 test, p Value=1, two-sided) **(A)**. Warts arising in wild-type and RB1^L mutant FVB/N mice share
626 similar microscopic features. Warts from both mouse genotypes were harvested, serially
627 sectioned, and stained with hematoxylin and eosin (H&E), processed to detect Ki67 (Ki67, red;
628 DAPI, blue) by immunofluorescence, and MCM7 by immunohistochemistry **(B)**.

629

630 **Figure 6. The C-terminal domain of RB1 is necessary for MmuPV1 E7 binding.**

631 Schematic representation of the RB1 protein and the expression plasmids used **(A)**. HA-epitope
632 tagged versions of full-length RB1, and the two truncation mutants 1-792 and 379-928 were
633 expressed in SAOS-2 human osteosarcoma cells in combination with FLAG/HA epitope-tagged
634 MmuPV1 (M E7) and HPV16 E7 (16 E7) expression vectors. After immunoprecipitation with
635 FLAG antibodies, HA-tagged E7 and co-precipitated RB1 proteins were detected by HA
636 immunoblot. The result shown is representative of two independent experiments. **(B)**.

637

638 **Figure 7. The RB1 binding site maps the MmuPV1 E7 C-terminus.** Sequence alignment

639 of the C-terminal domains of MmuPV1, canine papillomavirus 2 (CPV2), γ 1-HPV4, γ 24-HPV197,
640 β 1-HPV8, and α 9-HPV16 E7. Identical residues are marked by black boxes, chemically similar
641 residues are shaded in gray. The position of the CXXC motifs that form a zinc-binding site is
642 shown. The position of the aspartate residue at position 90 (D90) that is important for RB1
643 binding is indicated by a red box **(A)**. Various FLAG/HA-tagged MmuPV1 E7 mutants were
644 expressed in HCT116 cells and co-precipitated RB1 was detected by immunoblotting. The result
645 shown is representative of six independent experiments **(B)**. Immunoprecipitation western blot
646 analyses to assess RB1 binding by various MmuPV1 E7^{D90} mutants. The result shown is
647 representative of two independent experiments **(C)**. Immunoprecipitation/western blot analysis

648 documenting that MmuPV1 E7^{D90A} is defective for binding to murine Rb1. Wild type MmuPV1 E7
649 and the D90A mutant were transiently expressed in NIH3T3 cells and binding assessed by
650 immunoprecipitation/western blotting. The blot shown is representative of 2 independent
651 experiments **(D)**. Quantifications of E7-coprecipitated RB1 or Rb1 are normalized to the amount
652 of E7 that is precipitated and are shown underneath.

653

654 **Figure 8. MmuPV1 E7^{D90A} virus gives rise to reduced incidence and smaller-sized**
655 **warts than wild type MmuPV1.** To assess infectivity of quasivirus stocks, mouse JB6
656 keratinocytes were exposed to quasivirus and 48 hours later RNA was extracted and subjected
657 to reverse transcription-coupled polymerase chain reaction (RT-PCR) to detect MmuPV1 E1^{E4}
658 (top panel) or p53 (bottom panel) transcripts. Shown are results for mock-infected cells, and
659 cells infected with equal amounts of MmuPV1 derived from warts (positive control), wild type
660 MmuPV1 quasivirus (wild type), and two stocks of E7^{D90A} mutant quasivirus (E7^{D90A}) **(A)**. Wart
661 incidence arising at sites on nude mice infected with 10⁸ VGE of wild type MmuPV1 quasivirus,
662 10⁷ VGE of wild type MmuPV1 quasivirus as well as 10⁸ or 10⁷ VGE, respectively, of two
663 independent preparations of MmuPV1 E7^{D90A} quasivirus (E7^{D90A} Stock 1, E7^{D90A} Stock 2). The
664 incidence of warts at sites infected with MmuPV1 E7^{D90A} quasivirus was significantly less
665 compared to dose equivalent of wild type MmuPV1 quasivirus (Fisher's exact test, two-sided:
666 MmuPV1 (10⁸ VGE) vs. E7^{D90A} Stock 1, p<0.0001; MmuPV1 (10⁷ VGE) vs. E7^{D90A} Stock 2,
667 p<0.001). A dosage effect in wart formation was also observed with the wildtype MmuPV1
668 (MmuPV1 (10⁸ VGE) vs. MmuPV1 (10⁷ VGE), p=0.0001) **(B)**. Kaplan-Meier plot showing that
669 the percent of wart free sites over time is significantly different for MmuPV1 versus MmuPV1
670 E7^{D90A} quasivirus infections (LogRank test (two-sided): MmuPV1 (10⁸ VGE) vs. MmuPV1 E7^{D90A}
671 Stock 1, p<0.0001; MmuPV1 (10⁷ VGE) versus MmuPV1 E7^{D90A} Stock 2, p<0.0001; MmuPV1
672 (10⁸ VGE) versus MmuPV1 (10⁷ VGE), p<0.001) **(C)**. Representative images and of tails of mice
673 infected with the different quasiviruses at the 4 months endpoint (top images), along with equal

674 magnification of scanned images of sections of tails harboring representative warts stained with
675 H&E (bottom images) **(D)**. Size of warts at the 4 months endpoint. Warts arising from the
676 MmuPV1 E7^{D90A} quasivirus were significantly smaller (T-test, two-sided: MmuPV1 versus
677 MmuPV1 E7^{D90A}, p=0.003). Six MmuPV1 warts (three from each dose) and all three MmuPV1
678 E7^{D90A} quasivirus induced warts (two from Stock 1 and one from Stock 2) were used for this
679 quantification.

680

681 **Figure 9. MmuPV1 E7^{D90A} quasivirus-induced warts display similar histological**
682 **features as warts induced by wildtype MmuPV1.** Shown are serial sections of the mock-
683 infected tail (left column), and tail warts induced by wildtype MmuPV1 (middle column) or
684 MmuPV1 E7^{D90A} quasivirus (right column) stained with H&E **(A)**, stained for MmuPV1 L1 (red),
685 K14 (green) by immunofluorescence and counterstained with DAPI (blue) **(B)**, or
686 immunohistochemically stained for BrdU **(C)**, or MCM7 **(D)**.

687

688 **Table Legends:**

689

690 **Table S1:** Cellular proteins identified by Affinity purification/mass spectrometry (AP/MS) analyses of
691 carboxyl- or amino terminally epitope tagged MmuPV1 E7 (CE7 and NE7 respectively). The number of
692 unique and total peptides identified for each protein are shown. See reference [17] for experimental
693 details.

694

695 **Table S2:** Sequences of PCR primers used in this study.

696

697 **REFERENCES**

- 698 1. Van Doorslaer K, Li Z, Xirasagar S, Maes P, Kaminsky D, Liou D, Sun Q, Kaur R, Huyen Y, McBride
699 AA. 2017. The Papillomavirus Episteme: a major update to the papillomavirus sequence
700 database (pave.niaid.nih.gov). *Nucleic Acids Res* 45:D499-D506.
- 701 2. Schiffman M, Castle PE, Jeronimo J, Rodriguez AC, Wacholder S. 2007. Human papillomavirus
702 and cervical cancer. *Lancet* 370:890-907.
- 703 3. Chaturvedi AK, Engels EA, Pfeiffer RM, Hernandez BY, Xiao W, Kim E, Jiang B, Goodman MT,
704 Sibug-Saber M, Cozen W, Liu L, Lynch CF, Wentzensen N, Jordan RC, Altekrose S, Anderson WF,
705 Rosenberg PS, Gillison ML. 2011. Human papillomavirus and rising oropharyngeal cancer
706 incidence in the United States. *J Clin Oncol* 29:4294-301.
- 707 4. de Martel C, Ferlay J, Franceschi S, Vignat J, Bray F, Forman D, Plummer M. 2012. Global burden
708 of cancers attributable to infections in 2008: a review and synthetic analysis. *Lancet Oncol*
709 13:607-15.
- 710 5. Fuchs PG, Iftner T, Weninger J, Pfister H. 1986. Epidermodysplasia verruciformis-associated
711 human papillomavirus 8: genomic sequence and comparative analysis. *J Virol* 58:626-34.
- 712 6. Zachow KR, Ostrow RS, Faras AJ. 1987. Nucleotide sequence and genome organization of human
713 papillomavirus type 5. *Virology* 158:251-4.
- 714 7. Howley PM, Pfister HJ. 2015. Beta genus papillomaviruses and skin cancer. *Virology* 479-
715 480:290-6.
- 716 8. Meyers JM, Munger K. 2014. The viral etiology of skin cancer. *J Invest Dermatol* 134:E29-32.
- 717 9. Tommasino M. 2017. The biology of beta human papillomaviruses. *Virus Res* 231:128-138.
- 718 10. Vande Pol SB, Klingelutz AJ. 2013. Papillomavirus E6 oncoproteins. *Virology* 445:115-37.
- 719 11. Roman A, Munger K. 2013. The papillomavirus E7 proteins. *Virology* 445:138-68.
- 720 12. Moody CA, Laimins LA. 2010. Human papillomavirus oncoproteins: pathways to transformation.
721 *Nat Rev Cancer* 10:550-60.
- 722 13. Meyers JM, Grace M, Uberoi A, Lambert PF, Munger K. 2018. Inhibition of TGF-beta and NOTCH
723 Signaling by Cutaneous Papillomaviruses. *Front Microbiol* 9:389.
- 724 14. Spurgeon ME, Lambert PF. 2020. Mus musculus Papillomavirus 1: a New Frontier in Animal
725 Models of Papillomavirus Pathogenesis. *J Virol* 94.
- 726 15. Meyers JM, Uberoi A, Grace M, Lambert PF, Munger K. 2017. Cutaneous HPV8 and MmuPV1 E6
727 Proteins Target the NOTCH and TGF-beta Tumor Suppressors to Inhibit Differentiation and
728 Sustain Keratinocyte Proliferation. *PLoS Pathog* 13:e1006171.
- 729 16. Wang J, Zhou D, Prabhu A, Schlegel R, Yuan H. 2010. The canine papillomavirus and gamma HPV
730 E7 proteins use an alternative domain to bind and destabilize the retinoblastoma protein. *PLoS*
731 *Pathog* 6:e1001089.
- 732 17. Grace M, Munger K. 2017. Proteomic analysis of the gamma human papillomavirus type 197 E6
733 and E7 associated cellular proteins. *Virology* 500:71-81.
- 734 18. Xue XY, Majerciak V, Uberoi A, Kim BH, Gotte D, Chen X, Cam M, Lambert PF, Zheng ZM. 2017.
735 The full transcription map of mouse papillomavirus type 1 (MmuPV1) in mouse wart tissues.
736 *PLoS Pathog* 13:e1006715.
- 737 19. Pyeon D, Lambert PF, Ahlquist P. 2005. Production of infectious human papillomavirus
738 independently of viral replication and epithelial cell differentiation. *Proc Natl Acad Sci U S A*
739 102:9311-6.
- 740 20. Uberoi A, Yoshida S, Frazer IH, Pitot HC, Lambert PF. 2016. Role of Ultraviolet Radiation in
741 Papillomavirus-Induced Disease. *PLoS Pathog* 12:e1005664.

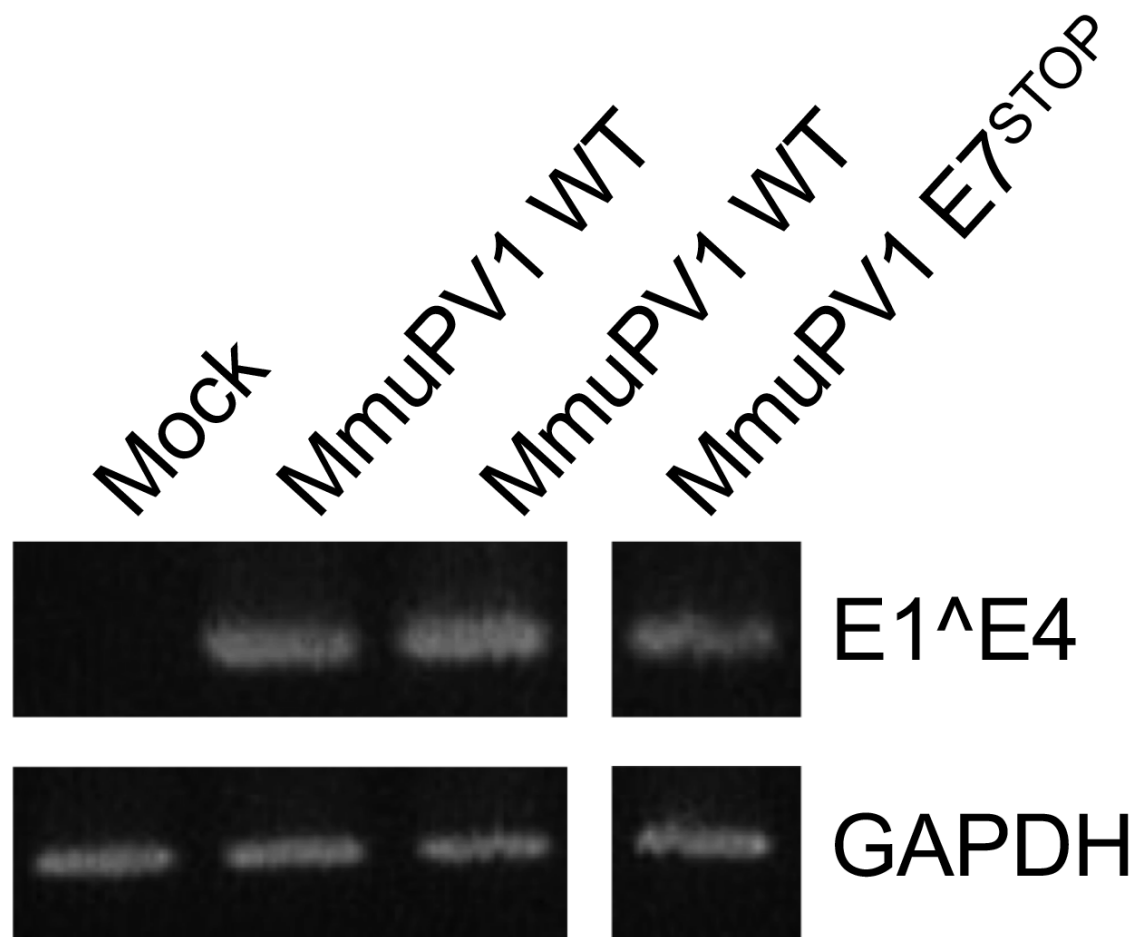
- 742 21. Cladel NM, Budgeon LR, Cooper TK, Balogh KK, Hu J, Christensen ND. 2013. Secondary infections,
743 expanded tissue tropism, and evidence for malignant potential in immunocompromised mice
744 infected with *Mus musculus* papillomavirus 1 DNA and virus. *J Virol* 87:9391-5.
- 745 22. Gonzalez SL, Stremlau M, He X, Basile JR, Munger K. 2001. Degradation of the retinoblastoma
746 tumor suppressor by the human papillomavirus type 16 E7 oncoprotein is important for
747 functional inactivation and is separable from proteasomal degradation of E7. *J Virol* 75:7583-91.
- 748 23. Shew JY, Lin BT, Chen PL, Tseng BY, Yang-Feng TL, Lee WH. 1990. C-terminal truncation of the
749 retinoblastoma gene product leads to functional inactivation. *Proc Natl Acad Sci U S A* 87:6-10.
- 750 24. Boyer SN, Wazer DE, Band V. 1996. E7 protein of human papilloma virus-16 induces degradation
751 of retinoblastoma protein through the ubiquitin-proteasome pathway. *Cancer Res* 56:4620-4.
- 752 25. Dyson N. 1998. The regulation of E2F by pRB-family proteins. *Genes Dev* 12:2245-62.
- 753 26. Nevins JR. 2001. The Rb/E2F pathway and cancer. *Hum Mol Genet* 10:699-703.
- 754 27. Weinberg RA. 1995. The retinoblastoma protein and cell cycle control. *Cell* 81:323-30.
- 755 28. Narasimha AM, Kaulich M, Shapiro GS, Choi YJ, Sicinski P, Dowdy SF. 2014. Cyclin D activates the
756 Rb tumor suppressor by mono-phosphorylation. *Elife* 3.
- 757 29. Sanidas I, Morris R, Fella KA, Rumde PH, Boukhali M, Tai EC, Ting DT, Lawrence MS, Haas W,
758 Dyson NJ. 2019. A Code of Mono-phosphorylation Modulates the Function of RB. *Mol Cell*
759 73:985-1000 e6.
- 760 30. Chellappan S, Kraus VB, Kroger B, Munger K, Howley PM, Phelps WC, Nevins JR. 1992.
761 Adenovirus E1A, simian virus 40 tumor antigen, and human papillomavirus E7 protein share the
762 capacity to disrupt the interaction between transcription factor E2F and the retinoblastoma
763 gene product. *Proc Natl Acad Sci U S A* 89:4549-53.
- 764 31. Lees E, Faha B, Dulic V, Reed SI, Harlow E. 1992. Cyclin E/cdk2 and cyclin A/cdk2 kinases
765 associate with p107 and E2F in a temporally distinct manner. *Genes Dev* 6:1874-85.
- 766 32. Leone G, DeGregori J, Yan Z, Jakoi L, Ishida S, Williams RS, Nevins JR. 1998. E2F3 activity is
767 regulated during the cell cycle and is required for the induction of S phase. *Genes Dev* 12:2120-
768 30.
- 769 33. Lee HH, Chiang WH, Chiang SH, Liu YC, Hwang J, Ng SY. 1995. Regulation of cyclin D1, DNA
770 topoisomerase I, and proliferating cell nuclear antigen promoters during the cell cycle. *Gene*
771 *Expr* 4:95-109.
- 772 34. Lee JO, Russo AA, Pavletich NP. 1998. Structure of the retinoblastoma tumour-suppressor
773 pocket domain bound to a peptide from HPV E7. *Nature* 391:859-65.
- 774 35. Dick FA, Sailhamer E, Dyson NJ. 2000. Mutagenesis of the pRB pocket reveals that cell cycle
775 arrest functions are separable from binding to viral oncoproteins. *Mol Cell Biol* 20:3715-27.
- 776 36. Balsitis S, Dick F, Dyson N, Lambert PF. 2006. Critical roles for non-pRb targets of human
777 papillomavirus type 16 E7 in cervical carcinogenesis. *Cancer Res* 66:9393-400.
- 778 37. Balsitis S, Dick F, Lee D, Farrell L, Hyde RK, Griep AE, Dyson N, Lambert PF. 2005. Examination of
779 the pRb-dependent and pRb-independent functions of E7 in vivo. *J Virol* 79:11392-402.
- 780 38. Brake T, Connor JP, Petereit DG, Lambert PF. 2003. Comparative analysis of cervical cancer in
781 women and in a human papillomavirus-transgenic mouse model: identification of
782 minichromosome maintenance protein 7 as an informative biomarker for human cervical cancer.
783 *Cancer Res* 63:8173-80.
- 784 39. Spurgeon ME, Uberoi A, McGregor SM, Wei T, Ward-Shaw E, Lambert PF. 2019. A Novel In Vivo
785 Infection Model To Study Papillomavirus-Mediated Disease of the Female Reproductive Tract.
786 *mBio* 10.
- 787 40. Joh J, Jenson AB, Proctor M, Ingle A, Silva KA, Potter CS, Sundberg JP, Ghim SJ. 2012. Molecular
788 diagnosis of a laboratory mouse papillomavirus (MusPV). *Exp Mol Pathol* 93:416-21.
- 789 41. Uberoi A, Lambert PF. 2017. Rodent Papillomaviruses. *Viruses* 9.

- 790 42. Patrick DR, Oliff A, Heimbrook DC. 1994. Identification of a novel retinoblastoma gene product
791 binding site on human papillomavirus type 16 E7 protein. *J Biol Chem* 269:6842-50.
- 792 43. Todorovic B, Hung K, Massimi P, Avvakumov N, Dick FA, Shaw GS, Banks L, Mymryk JS. 2012.
793 Conserved region 3 of human papillomavirus 16 E7 contributes to deregulation of the
794 retinoblastoma tumor suppressor. *J Virol* 86:13313-23.
- 795 44. Brandsma JL, Yang ZH, Barthold SW, Johnson EA. 1991. Use of a rapid, efficient inoculation
796 method to induce papillomas by cottontail rabbit papillomavirus DNA shows that the E7 gene is
797 required. *Proc Natl Acad Sci U S A* 88:4816-20.
- 798 45. Meyers C, Harry J, Lin YL, Wettstein FO. 1992. Identification of three transforming proteins
799 encoded by cottontail rabbit papillomavirus. *J Virol* 66:1655-64.
- 800 46. Haskell KM, Vuocolo GA, Defeo-Jones D, Jones RE, Ivey-Hoyle M. 1993. Comparison of the
801 binding of the human papillomavirus type 16 and cottontail rabbit papillomavirus E7 proteins to
802 the retinoblastoma gene product. *J Gen Virol* 74 (Pt 1):115-9.
- 803 47. Defeo-Jones D, Vuocolo GA, Haskell KM, Hanobik MG, Kiefer DM, McAvoy EM, Ivey-Hoyle M,
804 Brandsma JL, Oliff A, Jones RE. 1993. Papillomavirus E7 protein binding to the retinoblastoma
805 protein is not required for viral induction of warts. *J Virol* 67:716-25.
- 806 48. Qin XQ, Chittenden T, Livingston DM, Kaelin WG, Jr. 1992. Identification of a growth suppression
807 domain within the retinoblastoma gene product. *Genes Dev* 6:953-64.
- 808 49. Sellers WR, Rodgers JW, Kaelin WG, Jr. 1995. A potent transrepression domain in the
809 retinoblastoma protein induces a cell cycle arrest when bound to E2F sites. *Proc Natl Acad Sci U*
810 *S A* 92:11544-8.
- 811 50. Welch PJ, Wang JY. 1995. Disruption of retinoblastoma protein function by coexpression of its C
812 pocket fragment. *Genes Dev* 9:31-46.
- 813 51. Welch PJ, Wang JY. 1993. A C-terminal protein-binding domain in the retinoblastoma protein
814 regulates nuclear c-Abl tyrosine kinase in the cell cycle. *Cell* 75:779-90.
- 815 52. Ji P, Jiang H, Rekhtman K, Bloom J, Ichetovkin M, Pagano M, Zhu L. 2004. An Rb-Skp2-p27
816 pathway mediates acute cell cycle inhibition by Rb and is retained in a partial-penetrance Rb
817 mutant. *Mol Cell* 16:47-58.
- 818 53. Julian LM, Palander O, Seifried LA, Foster JE, Dick FA. 2008. Characterization of an E2F1-specific
819 binding domain in pRB and its implications for apoptotic regulation. *Oncogene* 27:1572-9.
- 820 54. Ishak CA, Marshall AE, Passos DT, White CR, Kim SJ, Cecchini MJ, Ferwati S, MacDonald WA,
821 Howlett CJ, Welch ID, Rubin SM, Mann MRW, Dick FA. 2016. An RB-EZH2 Complex Mediates
822 Silencing of Repetitive DNA Sequences. *Mol Cell* 64:1074-1087.
- 823 55. Binne UK, Classon MK, Dick FA, Wei W, Rape M, Kaelin WG, Jr., Naar AM, Dyson NJ. 2007.
824 Retinoblastoma protein and anaphase-promoting complex physically interact and functionally
825 cooperate during cell-cycle exit. *Nat Cell Biol* 9:225-32.
- 826 56. Dick FA, Goodrich DW, Sage J, Dyson NJ. 2018. Non-canonical functions of the RB protein in
827 cancer. *Nat Rev Cancer* 18:442-451.
- 828 57. Xiao B, Spencer J, Clements A, Ali-Khan N, Mittnacht S, Broceno C, Burghammer M, Perrakis A,
829 Marmorstein R, Gamblin SJ. 2003. Crystal structure of the retinoblastoma tumor suppressor
830 protein bound to E2F and the molecular basis of its regulation. *Proc Natl Acad Sci U S A*
831 100:2363-8.
- 832 58. Lee C, Chang JH, Lee HS, Cho Y. 2002. Structural basis for the recognition of the E2F
833 transactivation domain by the retinoblastoma tumor suppressor. *Genes Dev* 16:3199-212.
- 834 59. Joh J, Jenson AB, King W, Proctor M, Ingle A, Sundberg JP, Ghim SJ. 2011. Genomic analysis of
835 the first laboratory-mouse papillomavirus. *J Gen Virol* 92:692-8.

- 836 60. Kiyono T, Foster SA, Koop JI, McDougall JK, Galloway DA, Klingelhutz AJ. 1998. Both
837 Rb/p16INK4a inactivation and telomerase activity are required to immortalize human epithelial
838 cells. *Nature* 396:84-8.
- 839 61. Jeon S, Allen-Hoffmann BL, Lambert PF. 1995. Integration of human papillomavirus type 16 into
840 the human genome correlates with a selective growth advantage of cells. *J Virol* 69:2989-97.
- 841 62. Jeon S, Lambert PF. 1995. Integration of human papillomavirus type 16 DNA into the human
842 genome leads to increased stability of E6 and E7 mRNAs: implications for cervical carcinogenesis.
843 *Proc Natl Acad Sci U S A* 92:1654-8.
- 844 63. Chapman S, Liu X, Meyers C, Schlegel R, McBride AA. 2010. Human keratinocytes are efficiently
845 immortalized by a Rho kinase inhibitor. *J Clin Invest* 120:2619-26.
- 846 64. Spangle JM, Munger K. 2010. The human papillomavirus type 16 E6 oncoprotein activates
847 mTORC1 signaling and increases protein synthesis. *J Virol* 84:9398-407.
- 848 65. Baker SJ, Markowitz S, Fearon ER, Willson JK, Vogelstein B. 1990. Suppression of human
849 colorectal carcinoma cell growth by wild-type p53. *Science* 249:912-5.
- 850 66. Halbert CL, Demers GW, Galloway DA. 1991. The E7 gene of human papillomavirus type 16 is
851 sufficient for immortalization of human epithelial cells. *J Virol* 65:473-8.
- 852 67. Muller H, Lukas J, Schneider A, Warthoe P, Bartek J, Eilers M, Strauss M. 1994. Cyclin D1
853 expression is regulated by the retinoblastoma protein. *Proc Natl Acad Sci U S A* 91:2945-9.
- 854 68. Morgenstern JP, Land H. 1990. A series of mammalian expression vectors and characterisation
855 of their expression of a reporter gene in stably and transiently transfected cells. *Nucleic Acids*
856 *Res* 18:1068.
- 857 69. Longo PA, Kavran JM, Kim MS, Leahy DJ. 2013. Transient mammalian cell transfection with
858 polyethylenimine (PEI). *Methods Enzymol* 529:227-40.
- 859 70. Isaac CE, Francis SM, Martens AL, Julian LM, Seifried LA, Erdmann N, Binne UK, Harrington L,
860 Sicinski P, Berube NG, Dyson NJ, Dick FA. 2006. The retinoblastoma protein regulates pericentric
861 heterochromatin. *Mol Cell Biol* 26:3659-71.
- 862 71. Handisurya A, Day PM, Thompson CD, Buck CB, Kwak K, Roden RB, Lowy DR, Schiller JT. 2012.
863 Murine skin and vaginal mucosa are similarly susceptible to infection by pseudovirions of
864 different papillomavirus classifications and species. *Virology* 433:385-94.
- 865 72. Handisurya A, Day PM, Thompson CD, Buck CB, Pang YY, Lowy DR, Schiller JT. 2013.
866 Characterization of *Mus musculus* papillomavirus 1 infection in situ reveals an unusual pattern
867 of late gene expression and capsid protein localization. *J Virol* 87:13214-25.
- 868 73. Hopman AH, Ramaekers FC, Speel EJ. 1998. Rapid synthesis of biotin-, digoxigenin-,
869 trinitrophenyl-, and fluorochrome-labeled tyramides and their application for In situ
870 hybridization using CARD amplification. *J Histochem Cytochem* 46:771-7.

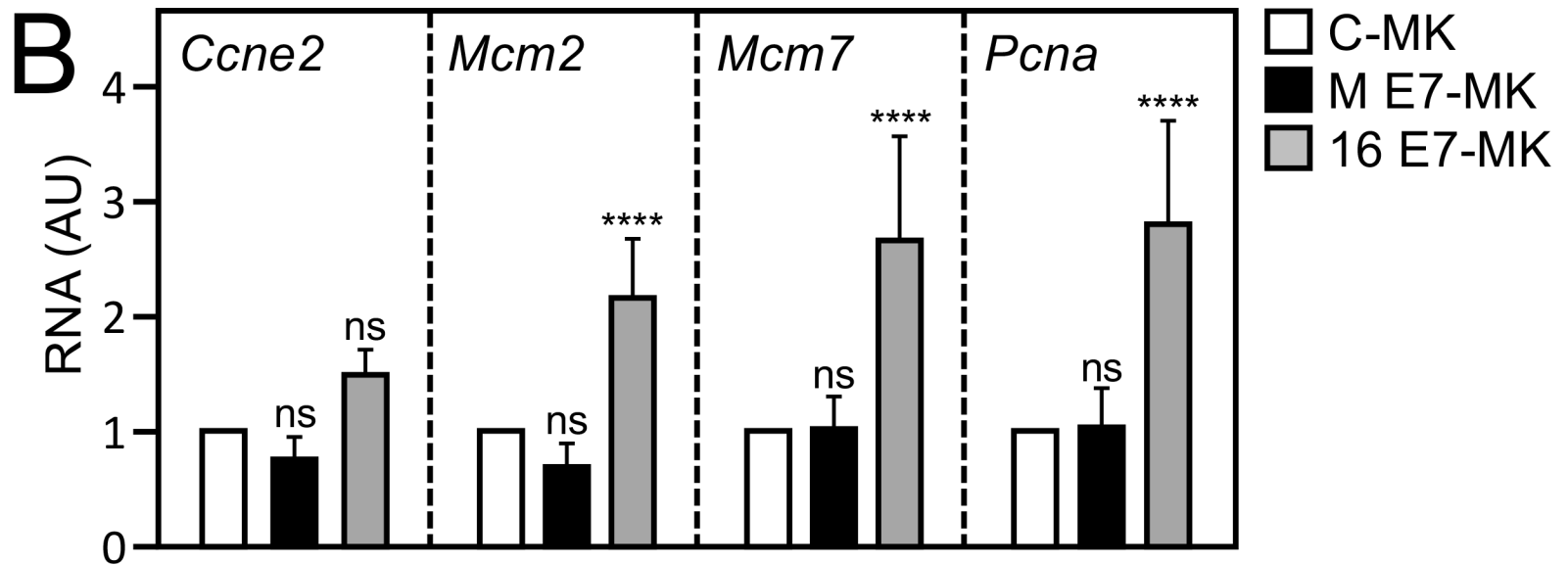
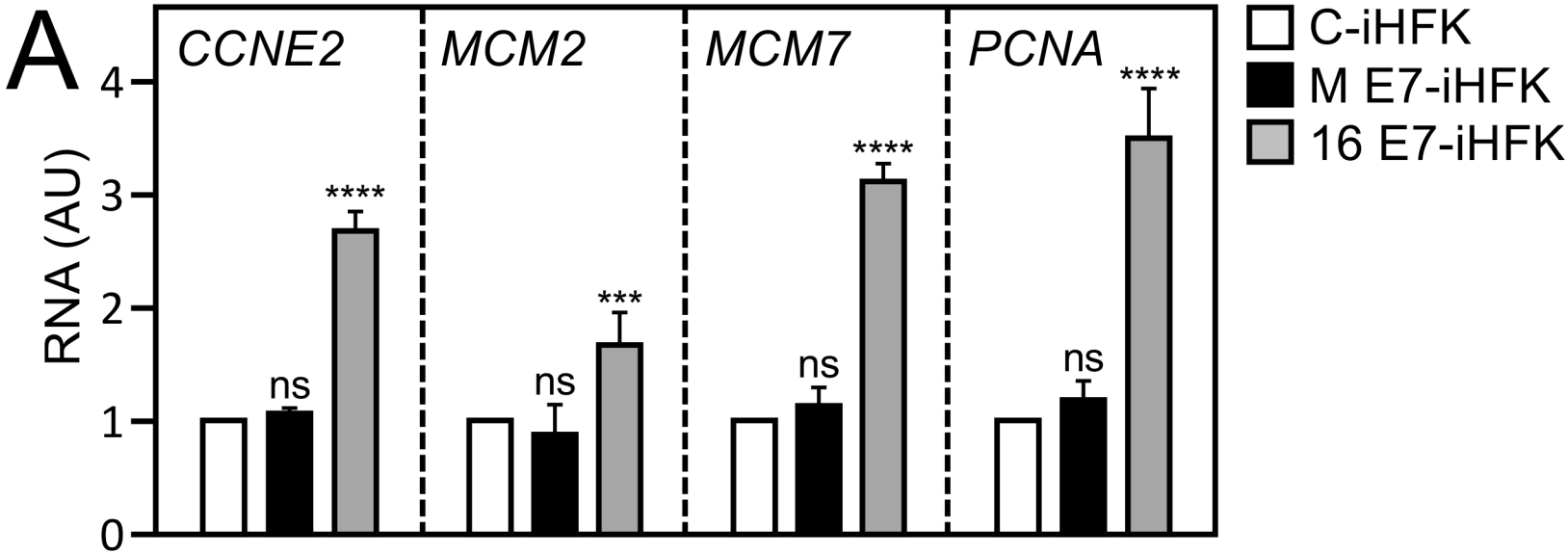
871

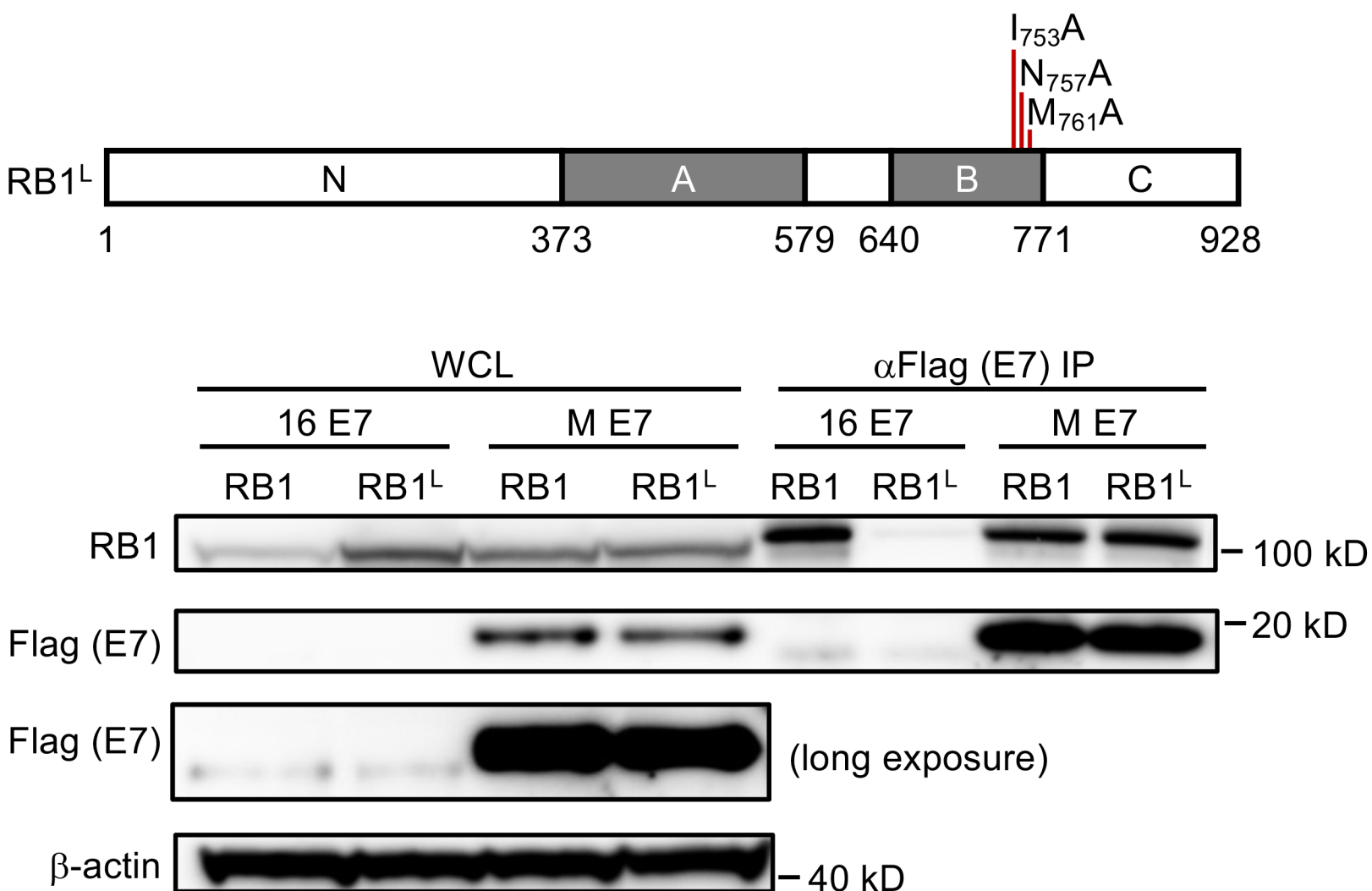
A



B

Genome	10 ⁸ quasivirus		10 μg DNA	
	# sites	# warts	# sites	# warts
MmuPV1	16	16	16	16
MmuPV1 E7 ^{STOP}	16	0	16	0





A

	# infected sites	# warts	incidence
FVB	26	16	62%
RB1^L mutant	22	13	59%

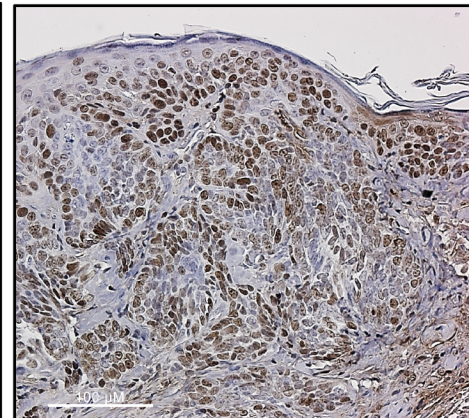
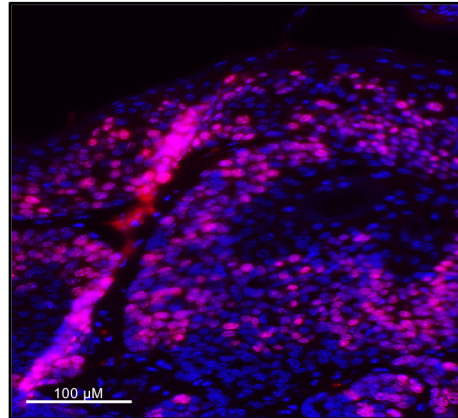
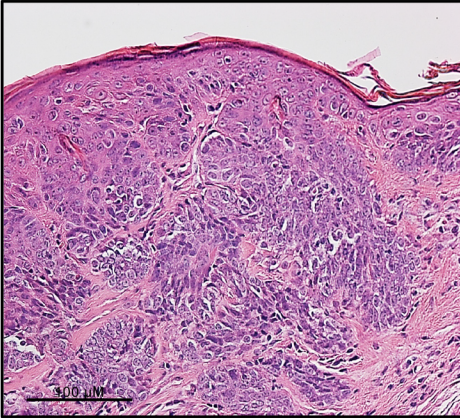
B

H&E

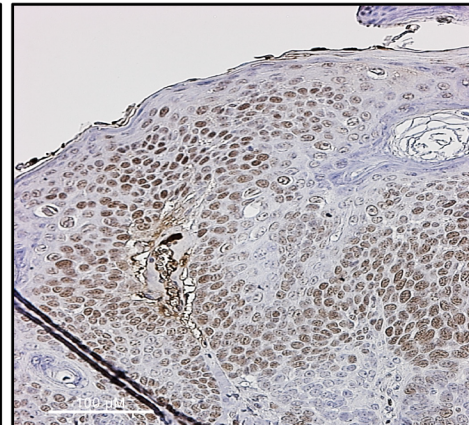
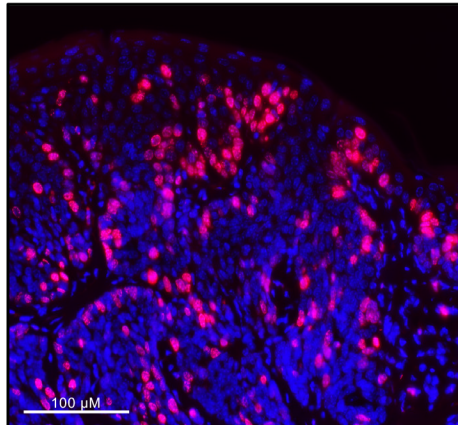
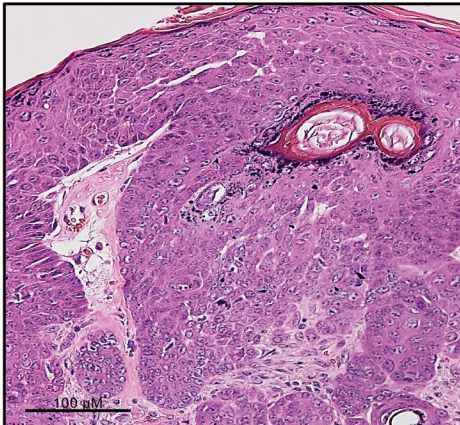
Ki67/DAPI

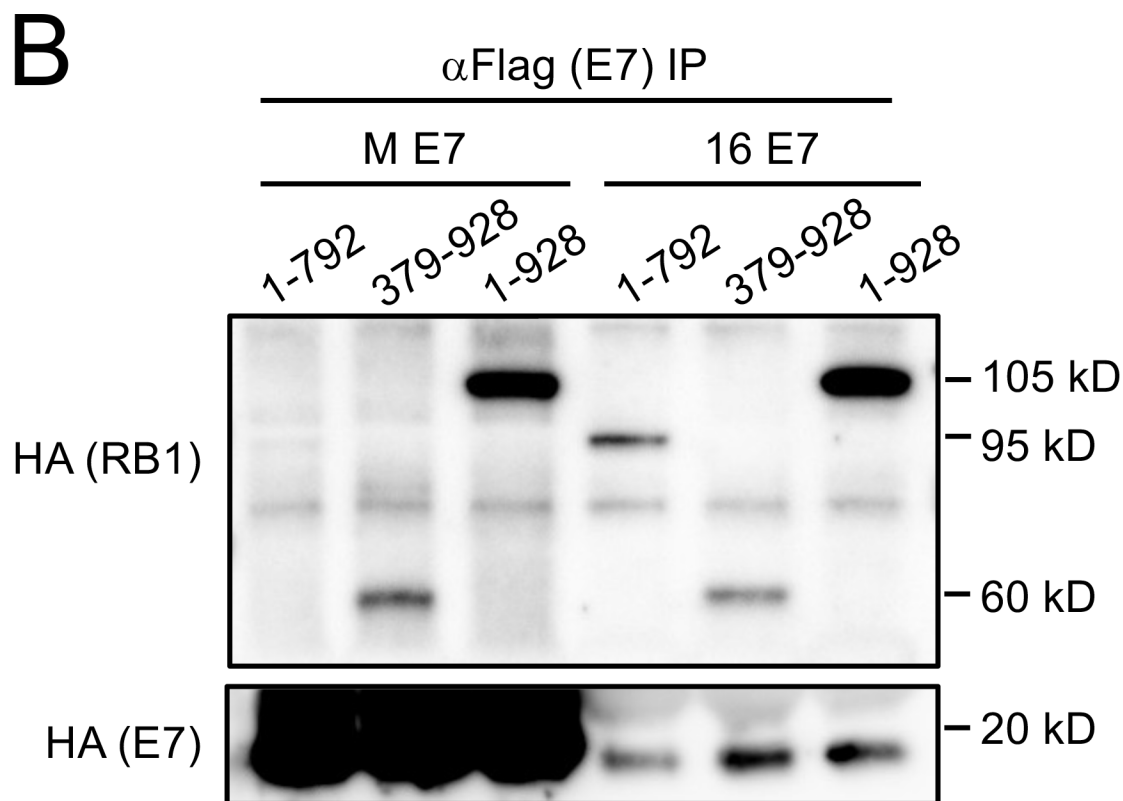
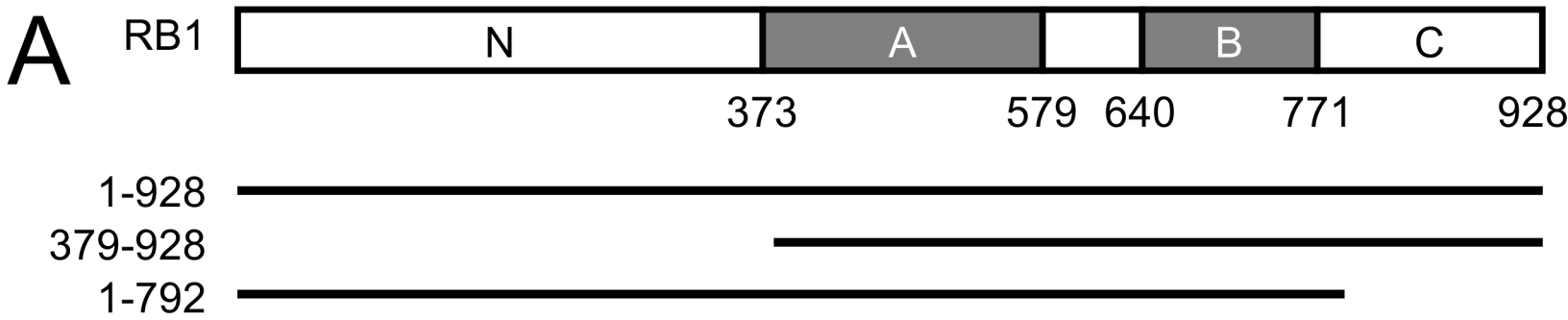
MCM7

FVB

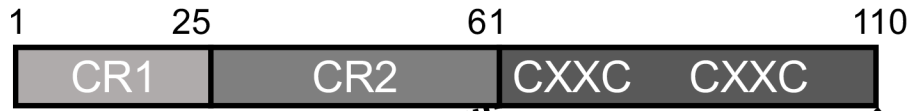


RB1^L





A

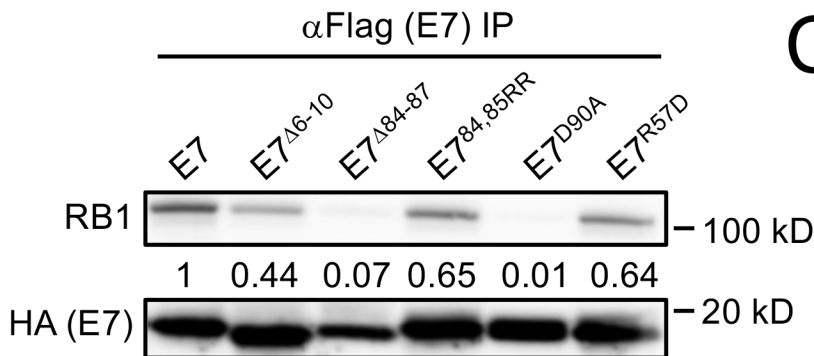


62 110

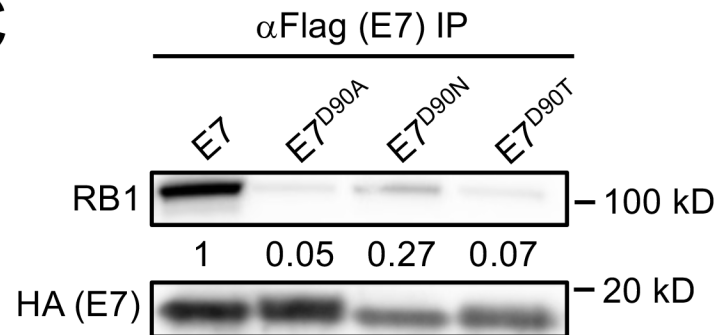
MmuPV1 E7 CFCCD TVLRFIIVTGDDSVKAFESLLLDQ-LSFVCPHCVASVYVNLNRNGKR
 CPV2 E7 CNICHSSLRLFVEVADESILIRLFQQLLDGLGIICATCHKEHFSDGRRR
 HPV4 E7 CYRCEVAVRITLYAAELGLRTLLEQLLVEGKLTFCCTACARS--LNRNGR
 HPV197 E7 CDNCRRGIRVVCVRASNQGISRLQWLEHD-IRFLCPACSRNLFQHGGRFQ
 HPV8 E7 CSCCQVKLRRLFVNATDSGIRTFQELLFRD-LQLLCPECRGNCKHGGG
 HPV16 E7 CCKCDSTLRRLCVQSTHVDIRTLLEDLLMGT-LGIVCPICISQKP

CXXC CXXC

B



C



D

